

Analysis of INS Derived Doppler Effects on Carrier Tracking Loop

Ravindra Babu, Jinling Wang

*School of Surveying and Spatial Information Systems
The University of New South Wales,
Sydney, NSW 2052
Australia*

Email: s.ravi@unsw.edu.au

Ph: +61-2-9385 4206

Fax: +61-2-9313 7493

Tracking dynamics on the GPS signal is still a big challenge to the receiver designer as the operating conditions are becoming more volatile. Optimizing the stand-alone system for dynamics, generally, degrades the accuracy of measurements. Therefore, an INS is integrated with GPS to address this issue. Doppler derived from INS can be used to aid the carrier tracking loop for improving the performance under dynamic conditions. However, the derived doppler does not truly reflect the GPS signal doppler due to errors in inertial sensors. As the tracking loop bandwidth is reduced significantly in Ultra-tightly integrated systems, any offsets in the aiding doppler creates undesired correlations in the tracking loop resulting in sub-optimal performance of the loop. The paper addresses this issue and also provides a mitigating mechanism to reduce the effects of incorrect estimates of the doppler. It is shown that doppler offsets resulting in a bias in the tracking loop can be appropriately modeled and removed. Mathematical algorithms pertaining to this are provided and the results are summarized. Simulations show that the bias due to aiding doppler offsets could be effectively addressed by appropriate modelling.

KEY WORDS

1. INS derived Doppler
2. Correlations
3. Stochastic Modelling

1. INTRODUCTION. Continuous tracking of GPS signals in dynamic scenarios pose a significant challenge for the design of the tracking loops. Optimizing a design to suit a particular scenario will degrade its performance in other scenarios. For instance, increasing the carrier tracking loop bandwidth to receive dynamic signals will inadvertently affect the accuracy of the raw measurements (Jwo, 2001; Cox, 1982). Therefore, in a stand-alone GPS receiver, a trade-off design is required to perform optimally in all the scenarios. External sensor integration with the GPS is considered as an alternative to improve upon this, and INS is the ideal choice as it is not only autonomous but also provides attitude at higher data rates.

Traditionally, the integration of GPS and INS were carried out in loosely and tightly coupled configuration (Brown & Hwang, 1997). While these systems offer significant advantages over the stand-alone GPS, nevertheless, it is imperative to improve the performance wherever possible. With this point of view, the development of integration presently culminated in Ultra-Tight Systems. This type of integration, also called deep level tracking, integrates the I (in-phase) and Q (quadrature) signals from the tracking loops of the GPS receiver with the Position and Velocity from INS (Sennott & Senffner, 1997). The primary advantage of this configuration, in addition to the benefits of loosely and tightly coupled systems, is a significant reduction of the carrier tracking loop bandwidth, as the doppler signal derived from INS aids the tracking loop to remove the dynamics from the GPS signals. Two important advantages stem from the reduction of the bandwidth: accuracy of the raw measurements, and immunity to jamming signals (Alban, 2003; Beser, 2002; Poh, et al., 2002; Kreye et al., 2000).

Unlike the loosely and tightly coupled systems, which are considered to be feed forward, ultra-tight systems are feedback systems, i.e., a feedback signal in the form of doppler derived from the INS also drives the tracking loops. For the successful implementation of this system, the accuracy of the doppler signal is very critical. The errors that degrade the doppler accuracy are the residual biases in the estimates of integration Kalman filter. It is well known that inertial sensors comprises of systematic and stochastic biases, which degrade the navigation solution (Titterton & Weston, 1997). Though the systematic bias is effectively removed by the integration Kalman filter by incorporating the GPS measurements, nevertheless, the stochastic component needs a different treatment. Appropriate modelling techniques, like Gauss Markov, Random-Walk and Autoregression effectively mitigate this noise (Nassar, 2003).

Conventional tracking loops get their feedback from within the channel. The Costas phase discriminator, which is the central part of the carrier-tracking loop, generates the corrections from I and Q measurements. These corrections, after filtering, drive the NCO (Numerically Controlled Oscillator), which generates the quadrature signals to reduce the error with the incoming signals. This configuration is suitable for a system with low dynamics. However, as the dynamics increase, the phase error transcends the threshold thereby loosing lock. Therefore, in the case of Ultra-tight receivers, the NCO gets its correction signal not only from within the channel, but also from the INS. This additional signal from the INS removes the dynamics from the GPS signal and subsequently keeps the loop in lock. The feedback from the INS is the key to the Ultra-tight receiver's performance.

Though the inertial aiding of the tracking loops seems to be attractive, if the aiding signal does not properly represent the true doppler, it results in a tracking loop bias, which degrades the phase output of the Costas discriminator. This phenomenon, which is unseen in stand-alone systems, is prevalent in ultra-tight receivers or receivers with doppler aiding. Ultimately, the challenge lies in removing any of the undesired effects created by the aiding signal. The paper discusses such effects and the remedial methods.

Figure 1 shows the block diagram of the Ultra-Tight Integrated System. The GPS receiver is Software based, and therefore, the acquisition and tracking loops entirely reside in Software. Though the Software receivers are comparatively slower than hardware based systems, they are still valuable, especially for development due to their flexibility (Brown, et al., 2000 & Chakravarthy et al., 2001; Tsui, 2000).

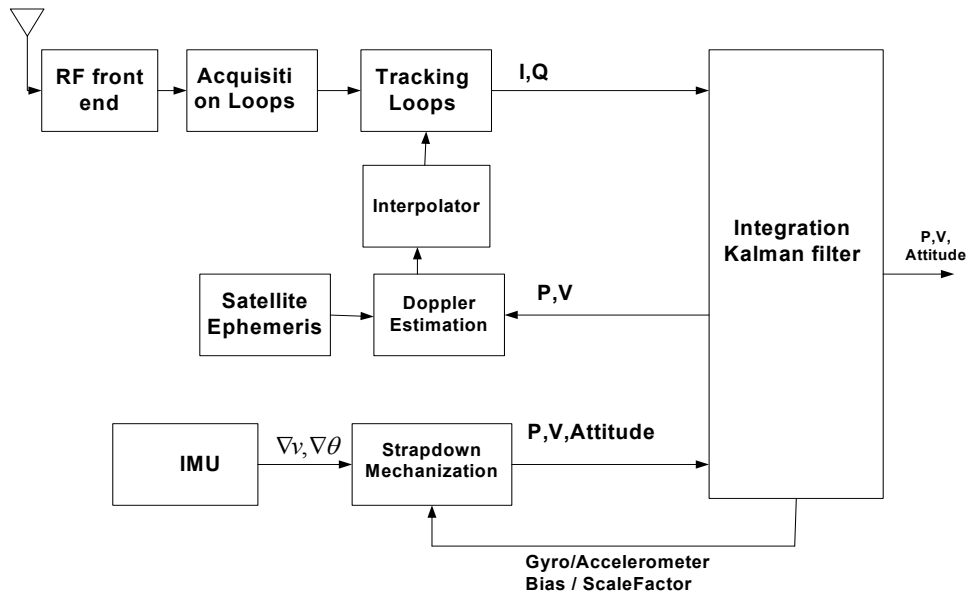


Figure 1 Block Diagram of Ultra-Tight Integration System

2. ULTRA-TIGHT CARRIER TRACKING LOOP ARCHITECTURE. Conventional receivers use two types of tracking loops to extract navigation data: code and carrier loop. Code loop despreads the incoming PRN code by multiplying with the locally generated code leaving only the data modulated carrier. Subsequently, the carrier-tracking loop, Costas Phase Locked Loop (CPLL), tracks on to the dynamics on the carrier and demodulates the data bits. The ability of the receiver to track dynamics depends on the bandwidth of the filter in CPLL. Increase in receiver dynamics results in an increase in doppler frequency on the carrier, and if the rate of change of doppler is more than the tracking loop bandwidth, then, eventually the PLL loses lock. To counteract this effect, if a redundant sensor such as an INS can measure and remove dynamics from GPS signals, then the CPLL can maintain lock even in dynamic scenarios. This is the method adopted in Ultra-tightly integrated GPS/INS receivers.

Typical unaided GPS receivers use a 2nd order carrier-tracking loop with a loop bandwidth of about 12 to 18Hz to receive a moderate dynamic signal. Excessive dynamics require the loop order to be increased to 3 to reduce the dynamic stress errors (Cahn, 1977; Ward, 1998; Isigler et al., 2002; Jwo, 2001). However, a 3rd order filter design is quite complex and also has potential stability problems. In ultra-tight systems, as dynamics from the GPS signal are removed by INS aiding, the filter order can be reduced to 2 and the bandwidth can still be maintained at about 3Hz. Further reduction in bandwidth is possible if an accurate receiver clock and a navigation-grade INS are used, but they are too expensive to be used in many commercial applications, forcing a limit on the bandwidth reduction. Figure 2 shows the block diagram of an inertially aided tracking loop. Unlike the conventional receivers, where the NCO is driven only by the phase discriminator output, in ultra-tight systems, the NCO is driven by two signals: phase discriminator output and the aiding signal. The distinguishing feature of Ultra-tight receiver is the feedback signal from the INS.

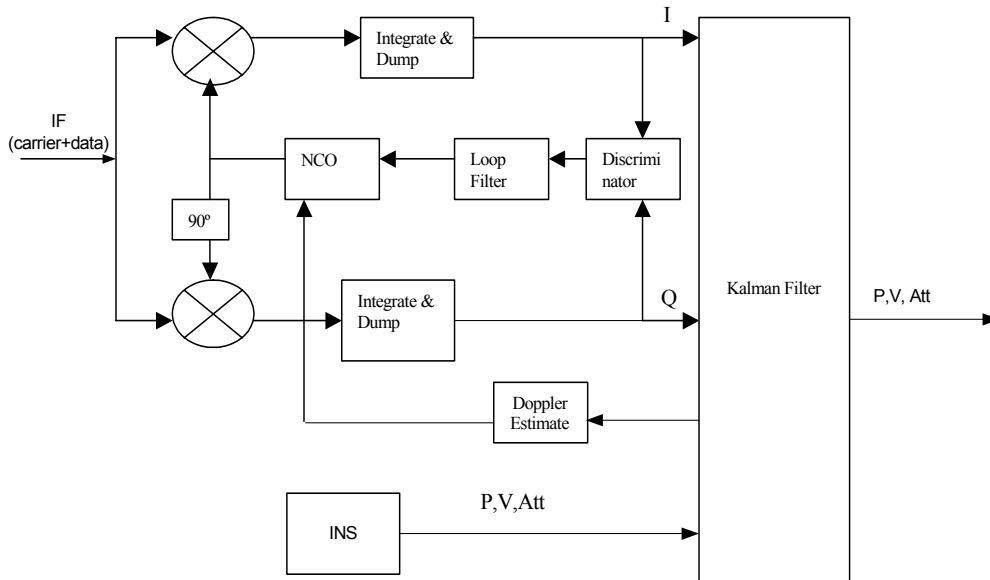


Figure 2. Carrier-Tracking Loop with Inertial Aiding

2.1. Tracking Loop Performance. The tracking performance of the ultra-tight loop is compared with a conventional loop in this section. The conventional loops have a limitation on the dynamics to be handled, and when the dynamics exceed the bandwidth, they switch back to wideband PLL or narrowband FLL (frequency lock loop) temporarily relinquishing the measurements for the navigation algorithm. However, ultra-tight tracking loops remain in the narrowband PLL mode even during high dynamics. Figure 3 shows the plot comparing the two loops with a constant velocity trajectory. While the conventional loops increase in frequency

with the input, the ultra-tight loops with a bandwidth of only 3Hz maintain almost a constant doppler. This property of maintaining a stable doppler irrespective of the input dynamics makes the ultra-tight systems attractive in dynamic applications.

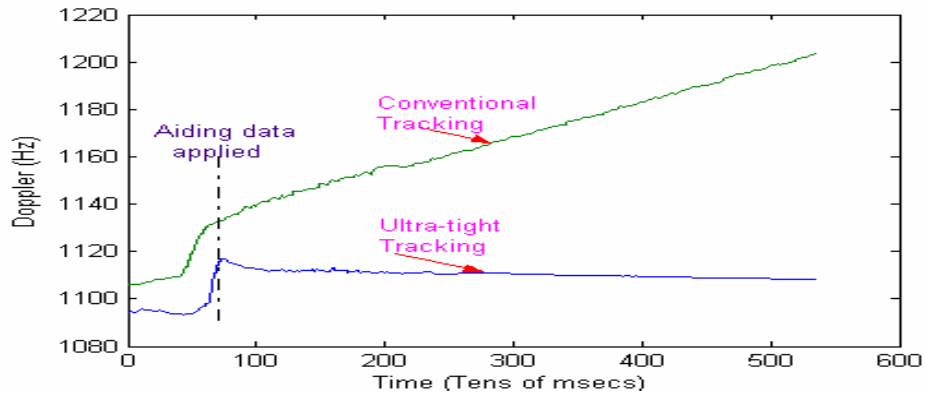


Figure 3 Conventional (BW = 13Hz) and Ultra-tight (BW = 3Hz) Doppler tracking performance

The feedback doppler signal removes most of the dynamics from GPS signals rendering the GPS signal to be ‘almost’ dynamic-free. So, any residual dynamics on GPS signals to be tracked is only due to the local oscillator. As the doppler due to oscillator is much less, carrier bandwidth can be reduced significantly to improve the accuracy of raw measurements. However, the quality of the aiding doppler signal is very important in such an integration mechanism, as any bias on this signal degrades the I and Q measurements. Figure 4 shows the components that contribute to the conventional and ultra-tight receiver bandwidths. In the case of conventional receivers, it is the receiver dynamics that occupies most part of the bandwidth; while in ultra-tight receivers, it is only the residual biases from the integration filter and the doppler from local oscillator that occupies the bandwidth.

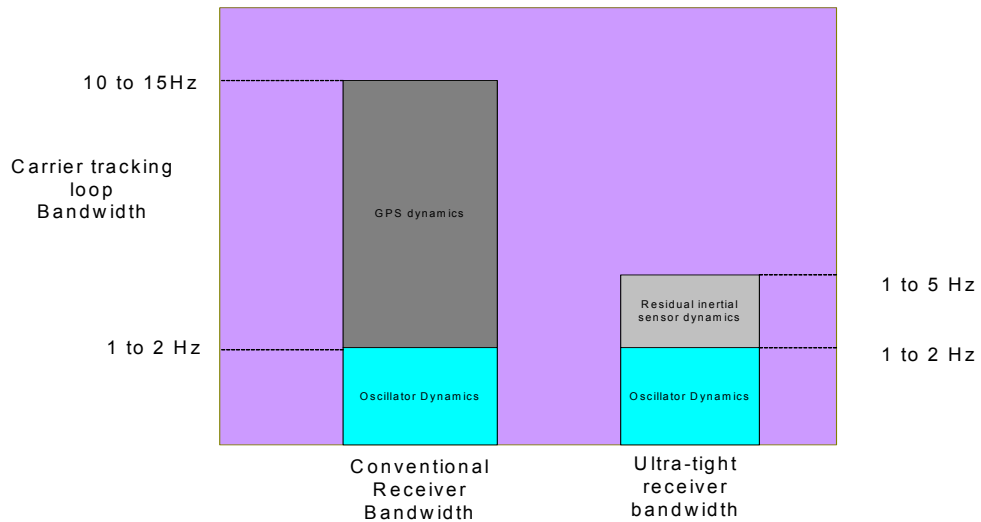


Figure 4 Conventional vs. Ultra-tight tracking loop bandwidth

3. BANDWIDTH AND DYNAMIC ANALYSIS. Consistent tracking of the doppler signal requires the bandwidth to be optimized continuously as the receiver passes through different environments. For instance, low dynamic environments require a carrier bandwidth of about 5 to 12 Hz, whereas high dynamic environments require a bandwidth greater than 18Hz. As the dynamics on the pseudorandom code is far less than on the carrier (code doppler is 1540 times less than on the carrier), the code tracking loop requires little optimization. At higher bandwidths, thermal noise degrades the accuracy of measurements. Unfortunately, both these requirements, higher bandwidth to receive high dynamics and low bandwidth to reduce the thermal error, cannot be optimized simultaneously for a stand-alone system. Therefore, a system designer should consider both thermal and dynamics effects in the tracking loop design.

However, external sensors can be integrated with the tracking loop for simultaneous optimization. Of the many possible sensors, INS (Inertial Navigation System) is the optimal choice, as not only it is autonomous, but it also provides attitude at higher data rates. Doppler information from INS can therefore be used to aid the tracking loops for removing dynamic stress from the GPS signal. With the extraction of receiver dynamics, the only component that remains to be tracked is the oscillator dynamics and this can be achieved with a considerably lower bandwidth.

Detecting a signal in the tracking loop requires a threshold to be set based on the statistical properties of the signal and thermal noise. Any degradation in the signal, caused by either excessive dynamics or reduction in signal strength, causes it to go below the threshold, and eventually lose lock. Therefore, a threshold should be set based on the loop bandwidth and expected dynamics on the signal. The 3-sigma errors that a carrier tracking loop can tolerate are

$$3\sigma_{PLL} = 3\sigma_t + \theta_e < 45 \text{ deg} \quad (1)$$

where

σ_t = the 1-sigma phase error due to thermal noise

θ_e = dynamic stress error

45 deg is the threshold below which the signal is assumed to be lost.

According to Kaplan (1996), the thermal noise and dynamic stress errors are given as

$$\sigma_t = \frac{360}{2\pi} \sqrt{\frac{B_n}{c/n_0} \left(1 + \frac{1}{2Tc/n_0}\right)} \quad (2)$$

$$\theta_e = 0.2809 \frac{\bar{a}}{B_n^2} (\text{deg}) \quad (3)$$

where

B_n = loop bandwidth in Hz

c/n_0 = carrier to noise ratio

T = pre-detection integration time (1msec)

\bar{a} = line-of-sight acceleration (m/s²)

Table 1 illustrates the errors at different dynamics and signal strengths. It is evident that as the dynamics increases the bandwidth required to reduce the errors also increases. For instance, at 0.1g the bandwidth can be maintained at 6Hz, whereas at 1g the bandwidth should be greater than 15Hz. The shaded blocks in the table represent the fact that the errors exceed the threshold and the tracking loop cannot maintain lock. Also, it can be inferred that the dynamics have a greater effect on the bandwidth than the thermal noise. Figure 5 shows the plot with 0.5g dynamics and signal strength of 27.5 dB-Hz.

Band width (Hz)	0.1g @ 30dB-Hz			0.5g @ 27.5dB-Hz			1g @ 25dB-Hz		
	Thermal Noise	Dynamic Error	Total Error	Thermal Noise	Dynamic Error	Total Error	Thermal Noise	Dynamic Error	Total Error
3	3.84	57.86	61.7	5.75	289.31	295.06	8.96	578.62	587.58
6	5.43	14.46	19.89	8.13	72.32	80.45	12.67	144.65	157.32
9	6.65	6.42	13.07	9.96	32.14	42.10	15.52	64.29	79.81
12	7.68	3.61	11.29	11.50	18.08	29.58	17.93	36.16	54.09
15	8.59	2.31	10.9	12.86	11.57	24.43	20.04	23.14	43.18
18	9.41	1.60	11.1	14.08	8.03	22.11	21.96	16.07	38.03

Table 1. PLL Tracking Errors

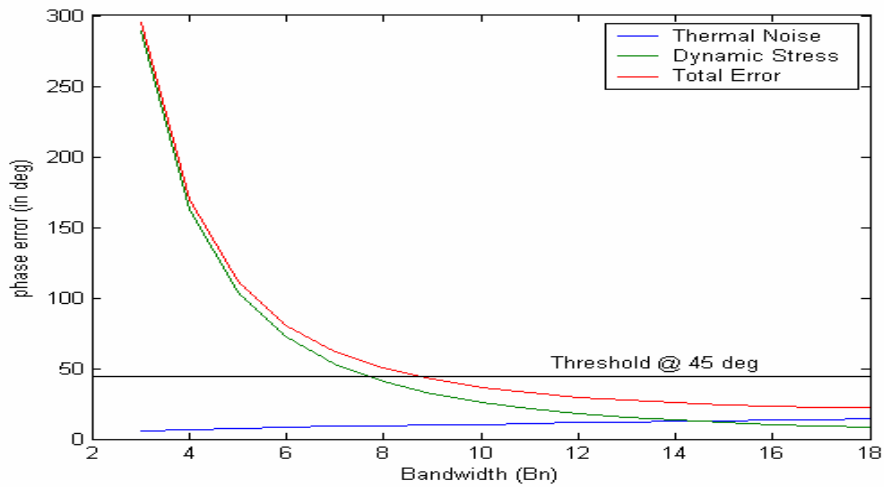


Figure 5 Thermal and Dynamic stress errors

4. DOPPLER ANALYSIS. As doppler is critical for ultra-tight systems, the doppler on both GPS carrier frequency and INS-derived are analysed here. Doppler, relative velocity between the transmitter and receiver, reflects the relative dynamics on the received RF (Radio frequency) carrier. As the dynamics of the GPS satellites are known accurately, velocity/acceleration information of the receiver can be extracted from the received doppler signal. The acquisition loops are almost immune to the doppler effects due to their higher bandwidth (+/- 500Hz for 1msec pre-detection integration), while the tracking loops are sensitive owing to their low bandwidth.

For simplified analysis, only the carrier with dynamics is considered; the pseudo-random code is assumed to be tracked and therefore can be ignored. The signal at the carrier-tracking loop is given as:

$$y(t) = A \sin(2\pi(f_{rel_vel} + f_{rxclk})t + \varphi) \quad (4)$$

where

- A = amplitude of the GPS signal
- f_{rel_vel} = Doppler frequency due to receiver dynamics
- f_{rxclk} = Doppler frequency due to clock
- φ = carrier phase at the phase detector

To track the signal shown in equation (4), the NCO generates two signals in quadrature. In a stand-alone receiver, corrections to the NCO are generated within the channel by a phase discriminator. However, in an aided configuration, corrections are generated from both the INS and the individual channel with a major contribution from INS. Let \hat{f}_{INS}^{dopp} be the doppler generated by the INS, and the NCO frequencies that drive the phase detector can be given as:

$$y_I(t) = \sin(2\pi \hat{f}_{INS}^{dopp} t + \theta) \quad (5)$$

$$y_Q(t) = \sin(2\pi \hat{f}_{INS}^{dopp} t + 90^\circ + \theta) \quad (6)$$

In equations (5) and (6), \hat{f}_{INS}^{dopp} is not the true doppler measured by the INS, but which is contaminated by the residual biases from the integration filter.

$$\hat{f}_{INS}^{dopp} = f_{INS}^{dopp} + f_{INS}^{resBias} \quad \text{and} \quad (7)$$

$$\begin{aligned} f_{INS}^{dopp} &= f^{tx} \left\{ 1 - \frac{v_{rel} \vec{a}}{c} \right\} \\ &= f_{rel_vel} \end{aligned} \quad (8)$$

where $f_{INS}^{resBias}$ is the residual bias from the navigation/integration filter, f^{tx} is the transmitted GPS frequency, v_{rel} is the relative velocity between the satellite and the INS, \vec{a} is the unit vector, and c is the velocity of light.

The phase detector multiplies the incoming signal in (4) with quadrature signals (5) & (6) generated by the NCO to give:

$$yy_I(t) = \cos(2\pi (f_{GPS}^{carr-dopp} - \hat{f}_{INS}^{dopp}) t) \quad (9)$$

$$yy_Q(t) = \cos(2\pi (f_{GPS}^{carr-dopp} - \hat{f}_{INS}^{dopp}) t + 90^\circ) \quad (10)$$

In equations (9) and (10)

$$f_{GPS}^{carr-dopp} = f_{rxclk} + f_{rel_vel} \quad (11)$$

where f_{rxclk} is the receiver clock offset, and f_{rel_vel} is the relative velocity between the satellite and the receiver. The higher frequency components generated in the mixing process are subsequently removed by the loop filter and therefore not mentioned here.

Substituting equations (7) and (11) into equations (9) and (10) gives the output of the phase detector:

$$yy_I(t) = \cos(2\pi (f_{rxclk} - f_{INS}^{resBias}) t) \quad (12)$$

$$yy_Q(t) = \cos(2\pi (f_{rxclk} - f_{INS}^{resBias}) t + 90^\circ) \quad (13)$$

Integrating equations (12) and (13) over the integration period T gives the I and Q measurements:

$$E[I] = \frac{A}{2f_{err}} \{ \cos(f_{err}(k+1)T) - \cos(f_{err}kT) \} \quad (14)$$

$$E[Q] = \frac{A}{2f_{err}} \{ \sin(f_{err}(k+1)T) - \sin(f_{err}kT) \} \quad (15)$$

where $f_{err} = f_{rxclk} - f_{INS}^{resBias}$ and E is the expectation operator.

Therefore, the effective doppler for the tracking loop to track is f_{err} , which is comparatively much lesser than the doppler on the signal (4) suggesting the fact that lesser bandwidth can be adopted if aiding is used. However, this is feasible only if the clock and the inertial sensors are accurate and stable. With lower accuracy clock and higher bias inertial sensors, the ultra-tight receivers lose their advantage. Moreover, f_{err} also affects the I and Q signals which are the measurements for the Kalman filter. These measurements, when integrated with the Position, Velocity and Attitude from INS in a Kalman filter, result in a sub-optimal performance. As the error from the clock is usually less, the doppler estimates from INS become a critical factor.

5. DISCRIMINATOR PHASE ERROR MODEL. Traditionally, carrier discriminator output is passed through a low-pass filter which drives the NCO (Kaplan, 1996; Tsui, 2000). The low-pass filter attenuates high frequency components and noise that result from the mixing process as mentioned before. This system architecture ensures optimal tracking as long as the measurements (I and Q) are not distorted. However, when correlation-induced biases distort the measurements, tracking performance starts to degrade (Sennott, 1992). This situation occurs in ultra-tight integration when the difference between the INS estimated Doppler and GPS Doppler exceeds the loop bandwidth which is typically about 3 to 5Hz. To reduce this undesired effect a Kalman filter based approach, discussed in the next section, is proposed.

A Costas tracking loop is used as a discriminator due to its insensitivity to 180° phase reversals in the I and Q data. It computes the phase error that is required to align internally generated signals to the incoming signal. The phase error generated by the discriminator is given by:

$$\varphi_{carr} = \tan^{-1} \left(\frac{Q_p}{I_p} \right) \quad (16)$$

where I_p and Q_p are in-phase and quadrature phase prompt channel outputs defined as (Kim et al, 2003, Sennott, 1999):

$$I_p = A R(\tau) D(t) \sin(\Delta\omega t + \theta) \quad (17)$$

$$Q_p = A R(\tau) D(t) \cos(\Delta\omega t + \phi) \quad (18)$$

where

$R(\tau)$ = Autocorrelation function of the PRN code

$D(t)$ = Navigation Data

$\Delta\omega$ = Frequency Variations

θ, ϕ = Phase components

$\Delta\omega$ in equations (17) & (18) represent the difference between the GPS and INS derived doppler. When this difference exceeds the bandwidth B_n (in equations 2 and 3), undesired correlation results in the phase error φ_{carr} . These correlations can be reasonably approximated with a random-walk process. The discrete time model for this is given by:

$$\varphi_{carr}[n] = \varphi_{carr}[n-1] + \varepsilon[n] \quad (19)$$

where $\varepsilon[n]$ is a zero mean Gaussian random noise, and 'n' is the present epoch. The phase error model is shown in Figure 6.

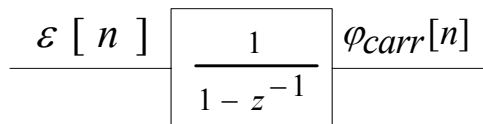


Figure 6 Discriminator Error Model

The discriminator output defined in equation (16) is plotted in figure 7 (a). After an initial transient, the phase error converges to a steady state value, which is a necessary criterion for the loop to be in lock. The autocorrelation plot shown in figure 7 (b) indicates that the signal is white and does not contain any correlations.

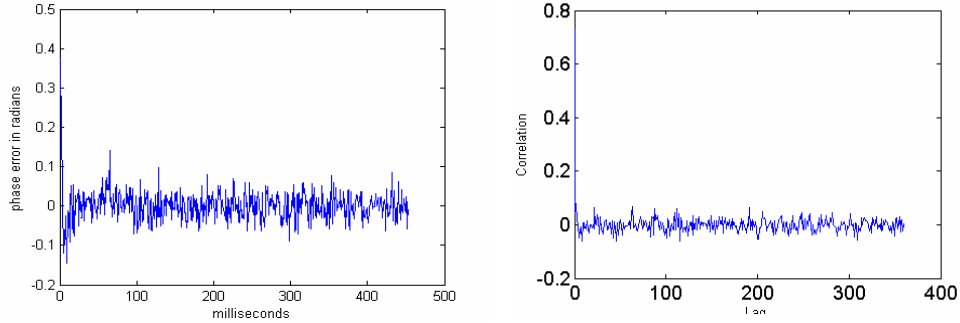


Figure 7 a) Phase Discriminator output b) Autocorrelation of discriminator output

6. A KALMAN FILTER BASED TRACKING LOOP. The proposed new signal tracking loop structure is shown in Figure 8. Instead of directly passing the loop filter’s output to the NCO, the signal is first corrected for any correlations in a Kalman filter. As shown in the figure, there are two inputs to the carrier NCO: one from within the channel generated by the phase discriminator, and other from the INS. The doppler estimate from INS is directly integrated with NCO output. As mentioned in the previous section, the INS estimated doppler offset induces a slowly changing bias in the tracking loop measurements which can be modeled as a random walk process.

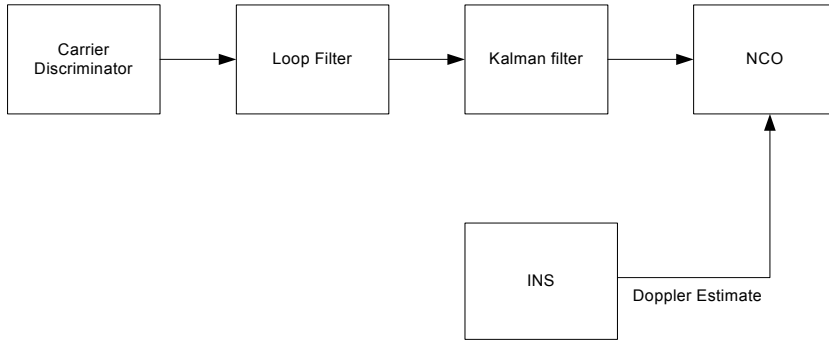


Figure 8 Kalman Filter based Tracking Loop

The correlations induced bias in the phase error can be represented as

$$E[\varphi_{carr}] \neq \varphi_{carr} \tag{20}$$

The state model of the Kalman filter implies that driving noise to the measurement and process models are Gaussian in nature. However, non-gaussian signals, like the phase discriminator in equation (20), can be modeled in the filter by augmenting the state vector. Therefore, in this problem, the two states considered are $x(k) = \{\hat{\varphi}_{carr}(k), \varphi_{carr}(k)\}$. While the first state represents the carrier phase, the second indicates the augmented random-walk.

Now, to optimally solve for the $\hat{\phi}_{carr}$, the process and measurement models are defined as below.

Process Model:

$$x[n] = Fx[n-1] + W_{carr}[n] \quad (21)$$

Measurement Model:

$$\varphi_{carr}[n] = Hx[n] + \gamma_{carr}[n] \quad (22)$$

where $W_{carr}[n]$ and $\gamma_{carr}[n]$ are the process and measurement noises respectively. The noise models that drive the process and measurement models are Q and R are:

$$Q = E[W_{carr}[n] W_{carr}[n]^T] \quad (23)$$

$$= \begin{bmatrix} 0 & 0 \\ 0 & w(k) \end{bmatrix} \text{ with } \text{var}(w(k)) = 5.0e-4$$

$$R = E[\gamma_{carr}[n] \gamma_{carr}[n]^T] \quad (24)$$

The propagation time in equation (21) is 1msec, and as the measurement and the state vector are the same, i.e. discriminator output, $H=1$. The process noise matrix $W_{carr}[n]$ is modeled with a random-walk driving process. Once the covariance matrix P and the state vector $\hat{\phi}_{carr}$ are initialized, the Kalman filter optimally estimates the discriminator signal. The flowchart for phase error model using the Kalman filter algorithm is shown in Figure 9

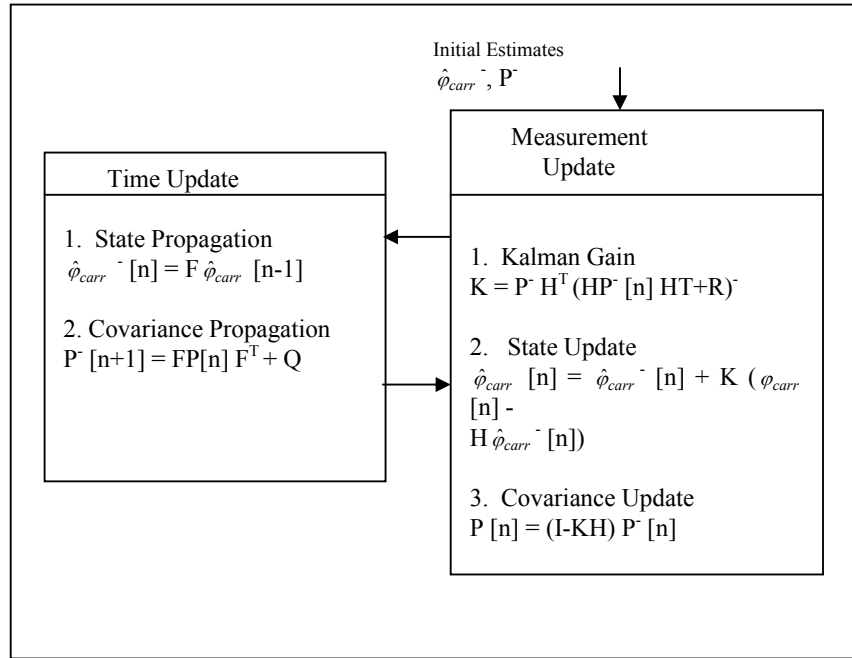


Figure 9 Kalman filter Model

7. SIMULATIONS & RESULTS. To evaluate the performance of the proposed tracking loop, simulations were carried out. The carrier tracking bandwidth is set at 3Hz, and a trajectory with known dynamics was given as input to both the Software Receiver and INS. Normally, due to systematic residual biases and any stochastic errors in the integration Kalman filter, the INS-estimated Doppler will not represent the true value. Based on the grade of INS, error in the

estimated Doppler can vary significantly. Two scenarios are presented to illustrate the performance: a 5 Hz offset, and a 10 Hz offset in the INS derived Doppler. Each experiment was carried out twice; once with a conventional Ultra-tight tracking loop, and with the modified tracking loop (with the inclusion of Kalman filter) during the subsequent run.

Test 1:

The first experiment was carried out with the INS estimated Doppler within 5 Hz of the true Doppler. This level of accuracy can be achieved with a tactical grade INS with a gyro bias better than 1deg/hr. Due to the doppler offset, the phase discriminator output shows correlations. A correlation analysis was also performed to check for any trend due to the bias in the estimated Doppler frequency, and the results are plotted in Figure 10. Figure 10 (a) shows the phase discriminator output, which drives the NCO via a loop filter. The autocorrelation plot in figure 10 (b) shows the correlations in the discriminator output.

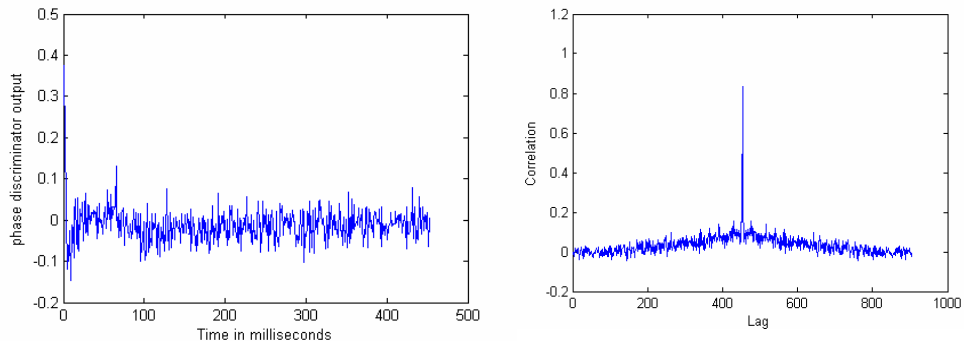


Figure 10 Ultra-tight tracking loop performance a) Phase Discriminator Output b) Autocorrelation

The same experiments were carried out with a Kalman filter introduced in the tracking loop modeled with a random walk, and the results are plotted in Figure 11. The phase error and correlation plot indicates that the filter effectively removes the correlations.

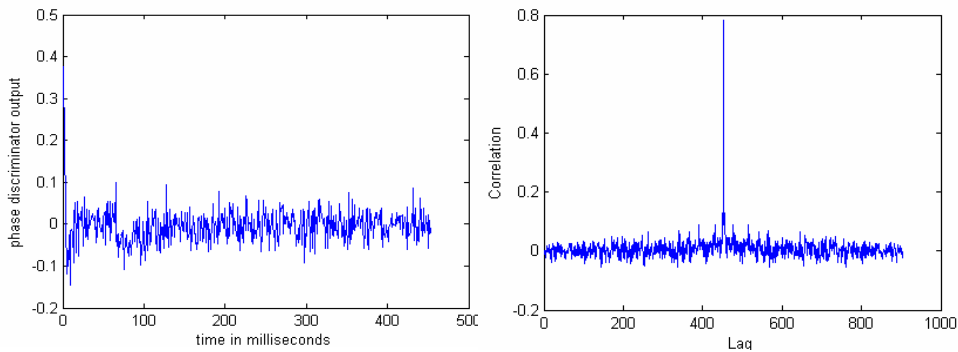


Figure 11 Modified Ultra-tight tracking loop performance a) Discriminator Output b) Autocorrelation

Test 2:

The next set of experiments was carried out with an INS estimated Doppler error about 10 Hz offset from the true value and the discriminator output and its autocorrelation are plotted in Figure 12. As the doppler differences increases, so do the correlations as shown in Figure 12 (b). However, when the same experiment was carried out with the Kalman filter included, these correlations were mitigated as shown in figure 13.

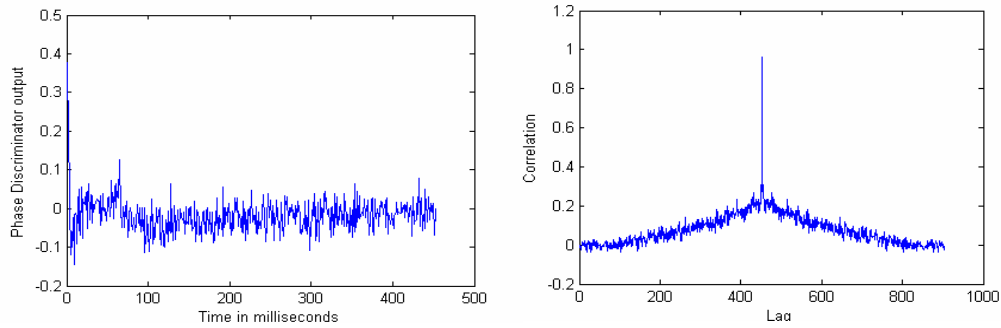


Figure 12 Ultra-tight tracking loop performance a) Discriminator Output b) Autocorrelation

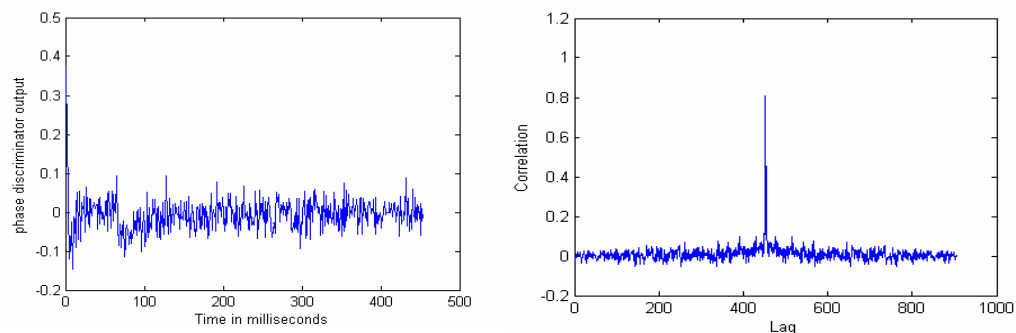


Figure 13 Modified Ultra-tight tracking loop performance a) Discriminator Output b) Autocorrelation

From the above two tests, it can be concluded that offsets in the aiding signal within a reasonable limits (<10Hz) can be successfully mitigated using the modified tracking loop approach. The correlogram analysis proves this supposition. However, the same methodology cannot be adopted if the offsets exceed 10 Hz.

8. CONCLUDING REMARKS

The standard tracking loop structure was shown to exhibit correlations due to inaccuracies in the INS derived doppler signal. This, in turn, biases the phase discriminator output and subsequently the I and Q outputs. When these I and Q measurements are incorporated in the integration Kalman filter, it results in a sub-optimal performance. Though the bias can be modeled in the state space of the integration filter, it nevertheless increases the system complexity. Two options were suggested to address this issue: using a high grade INS and a better than 0.1ppm oscillator, or modeling techniques. As the latter is cost-effective and also a flexible approach, a Kalman filter modeling approach was chosen to mitigate the undesired effects due to aiding in the tracking loops.

The performance of the standard ultra-tight tracking loop was compared with the modified structure and the results are summarized. The proposed loop shows a significant improvement by effectively removing the correlations. In addition, with less number of state variables the computation load is not much and this algorithm can be implemented in real-time with minimal computational load. The concepts of ultra-tight integration and the algorithms for the proposed tracking loop structure have been described. The results of preliminary investigations are encouraging and this method may prove to be an attractive solution, especially when using low cost inertial sensors.

ACKNOWLEDGEMENTS

This research is supported by an ARC (Australian Research Council) – Discovery Research Project on ‘Robust Positioning Based on Ultra-tight integration of GPS, Pseudolites and inertial sensors’.

REFERENCES

Alban, S., Akos, D., Rock, S., & Gebre-Egziobher, D., (2003) Performance Analysis and Architectures for INS-Aided GPS tracking loops. *Institute of Navigation – NTM*, Anaheim, CA, 22-24 January, 611-622.

Beser, J., Alexander, S., Crane, R., Rounds, S., Wyman, J., & Baeder, B., (2002) TrunavTM: A Low-Cost Guidance/Navigation Unit Integrating a SAASM-based GPS and MEMS IMU in a Deeply Coupled Mechanization. *15th Int. Tech. Meeting of the Satellite Division of the U.S. Inst. of Navigation*, Portland, Oregon, 24-27 September, 545-555.

Brown, R.G., & Hwang, P.Y.C., (1997) *Introduction to Random Signals and Kalman Filtering*. 3rd edition, John Wiley & Sons, NY.

Brown, A., May, M., & Tanju, B., (2000) Benefits of Software GPS receivers for Enhanced Signal Processing. *GPS Solutions*, 4, 56-66.

Cahn, R.C., Leimer, D.K., Marsh, C.L., Huntowski, F.J., Larue, G.D., (1977) Software Implementation of a PN Spread Spectrum Receiver to Accommodate Dynamics. *IEEE Transactions on communications*, 25 (8) pp.832-839.

Cox, D.B., (1982) Integration of GPS with Inertial Navigation Systems. *Navigation, Journal of the Institute of Navigation*, 1, 144-153.

Chakravarthy, V., Tsui, J.B.Y., & Lin, D.M., (2001) Software GPS Receiver. *GPS solutions*, 5, 63-70.

Irsigler, M., & Eissfeller, B., (2002) PLL Tracking Performance in the Presence of Oscillator Phase Noise. *GPS Solutions*, 5, 45-57.

Jwo D.-J., (2001) Optimization and Sensitivity Analysis of GPS Receiver Tracking Loops in Dynamic Environments. *IEE Proceedings of Radar, Sonar Navigation*, 148, 241-250.

Kaplan, E.D., (1996) *Understanding GPS: Principles and Applications*. Artech House, MA.

Kim, H., Bu, S., Jee, G., & Chan-Gook, P., (2003) An Ultra-Tightly Coupled GPS/INS Integration Using Federated Kalman Filter. *16th Int. Tech. Meeting of the Satellite Division of the U.S. Inst. of Navigation*, Portland, Oregon 9-12 September, 2878-2885.

Kreye, C., Eissfeller, B., & Winkel, J.O., (2000) Improvements of GNSS Receiver Performance Using Deeply Coupled INS Measurements. *13th Int. Tech. Meeting of the Satellite Division of the U.S. Inst. of Navigation*, Salt Lake City, Utah, 19-22 September, 844-854.

Nassar, S., (2003) Improving the Inertial Navigation System (INS) Error Model for INS and INS/DGPS Applications. *PhD Thesis*, University of Calgary, Canada.

Poh, E-K., Koh, A., & Wong, G., (2002) Evaluation of Coupled GPS/INS Integration Using Software GPS Receiver Model. *15th Int. Tech. Meeting of the Satellite Division of the U.S. Inst. of Navigation*, Portland, Oregon, 24-27 September, 2443-2450.

Sennott, J.W., & Senffner, D., (1992) The Use of Satellite Geometry for Prevention of Cycle Slips in a GPS Processor. *Navigation, Journal of the Institute of the Navigation*, 39, 217-235.

Sennott, J., & Senffner, D., (1997) Robustness of Tightly Coupled Integrations for Real-Time Centimeter GPS Positioning. *10th Int. Tech. Meeting of the Satellite Division of the U.S. Inst. of Navigation*, Kansas City, Missouri, 16-19 September, 655-663.

Sennott, J., (1999) Receiver Architectures for Improved Carrier Phase Tracking in Attenuation, Blockage, and Interference. *GPS solutions*, 3, 40-47.

Titterton, D.H., & Weston, J.L., (1997) *Strapdown Inertial Navigation Technology*. Stevenage, U.K., Peregrinus.

Tsui, J.B.Y., (2000) *Fundamentals of Global Positioning Receivers – A Software Approach*. John Wiley & Sons, Inc.

Ward, P., (1998) Performance Comparisons Between FLL, PLL and a Novel FLL-Assisted PLL Carrier Tracking Loop Under RF Interference Conditions. *11th Int. Tech. Meeting of the Satellite Division of the U.S. Inst. of Navigation*, Nashville, Tennessee, 15-18 September, 783-795.